A Miniaturized Printed Circuit CRLH Antenna-based Hilbert Metamaterial Array

Marwa M. Ismail, Taha A. Elwi, and A. J. Salim

***Abstract*—With the development of communication systems and antennas, various challenges arise that require antennas of small size with enhanced performance. Metamaterials (MTM) defects introduced a considerable solution to such a challenge. Therefore, in this paper, a lightweight with low profile antenna is designed based on a novel design of a Composite Right/Left-Handed CRLH-MTM Hilbert array. The proposed CRLH-MTM unit cell consists of a T-symmetric CRLH unit cell conjugated to the 3rd-order Hilbert on the ground plane through a T-stub structure to enhance the gain-bandwidth product. CST-MWS is used to stimulate and design the proposed antenna structure. The antenna parameters are optimized to evaluate the antenna performance in gain and S_{11}. As a result, the antenna can operate forward and backwards with a large scanning angle ranging from +34º to -134º with changing frequency, and dual-band extended from 3.3GHz to 4.2GHz 4.86GHz 5.98GHz with a maximum gain of 7.24dBi and 3.74dBi, respectively. The beam steering is achieved by trough controlling the switching operation of PIN diodes. As a result, the antenna can scan up to 8° from 34° to 42° at 3.5GHz with constant gain along with the operating range.**

***Index terms*—CRLH, Hilbert curve, Metamaterial, Reconfigurable antenna, Miniaturized Printed Circuit.**

I. INTRODUCTION

Communication systems were developed rapidly [1]. To keep up with this development, it has become necessary to manufacture antennas characterized by their small size, high efficiency and scan-ability [2]. Various techniques have been used to achieve these requirements. Meta-materials (MTM) are the most important technologies used in this field [3-5]. MTMs are scientifically defined as materials that meet the requirements of effective homogeneity and possess unique properties not found in nature [6]. Such technology started in 1967. when Victor Veselago predicted the existence of materials with negative permeability and permittivity. Veselago called it LH-MTM because it generates a left-handed propagation, different from available materials that create a right-handed triad [7, 8]. However, these materials were considered theoretical and could not be constructed due to the natural effects generated when current passes through the medium structure [9].

Consequently, there is no truly left-handed structure in nature [10]. Instead, the natural physical interactions passing through the material combine the characteristics of the right-handed and left-handed MTMs to produce a new type of MTM called CRLH-MTM. Caloz and Itoh introduced this type, which considered the general and most comprehensive form of LH-MTMs [11, 12]. The CRLH consist of series capacitance and shunt inductance, as shown in Fig. 1, and can be constructed using Surface-Mount Technology (SMT) or distributed components.

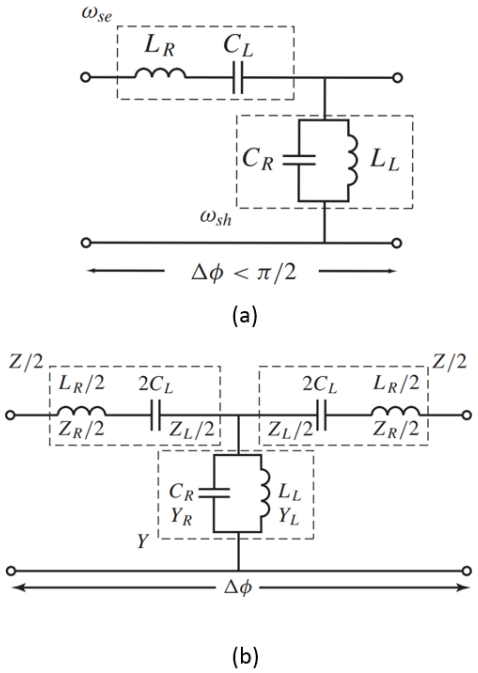

Fig. 1. CRLH- MTMs. (a) asymmetric CRLH unit cell (b) T-symmetric CRLH unit cell

CRLH is widely used in many applications to improve gain, increase bandwidth, and manufacture low-complexity systems [13, 14]. In [15], a printed array was constructed based on substrate-integrated waveguide SIW technology combined with slots and via techniques of high millimetre-wave bands with ±30° scanning angle with a gain of 8.5 dBi. Synthetic material was designed to achieve negative electromagnetic characteristics over a wide range of frequencies. In [16], an artificial material has been designed and tested to detect gap-free and gap transitions. The manufactured material provides

Manuscript received April 6, 2022; revised May 26, 2022. Date of publication July 5, 2022. Date of current version July 5, 2022. The associate editor prof. Zoran Blažević has been coordinating the review of this manuscript and approved it for publication.

M. M. Ismail and A. J. Salim are with the Department of Electrical Engineering, University of Technology, Baghdad, Iraq (eee.19.06@grad.uotechnology.edu.iq, ali.j.salim@uotechnology.edu.iq).

T. A. Elwi is with the Department of Communication Engineering, Al-Ma 'moon University College, Baghdad, Iraq (taelwi82@gmail.com).

Digital Object Identifier (DOI): 10.24138/jcomss-2022-0030

double negative parameters at low frequencies and double-positive parameters at high frequencies. The transition from negative to positive occurs at the same resonant frequency, thus providing a balanced CRLH. In [17], a new half-width LWA was presented in this work; it had the ability to continue directing the main lobe with a swap frequency; through the introduction of vertical and horizontal slots within the radiation element, the operating frequency was swept between 4 to 6 GHz with a maximum gain of 10 dBi at 4.3 GHz. In [18], an antenna was manufactured using CRLH MTM technology to increase the impedance bandwidth without affecting the antenna size, with frequencies ranging from 850 MHz to 7.90 GHz. A CRLH antenna with broadband scanning capability was proposed in [19] using identical transmission line sections inserted into the cell with limited bandwidth.

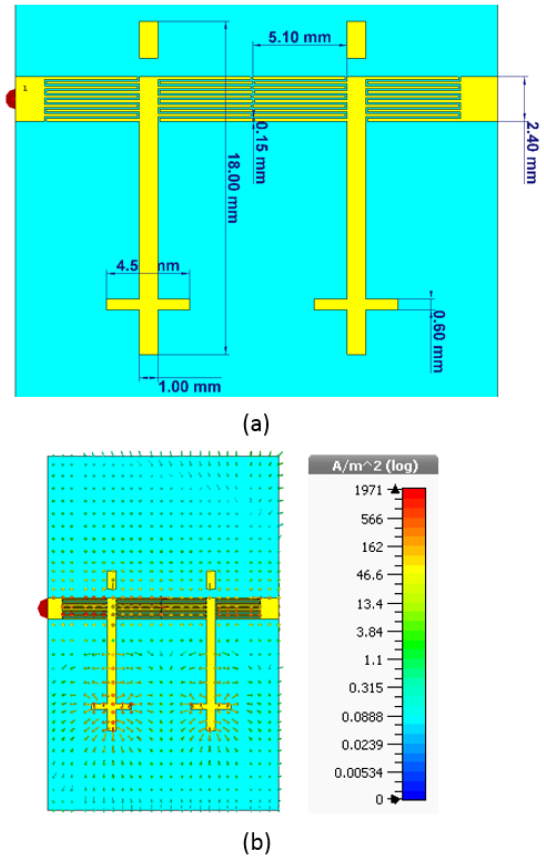

Fig. 2. Unit cell design (a) CRLH- MTM geometrical details (b) current density.

A frequency scanning antenna array is designed in [20]; the CRLH unit cell is used as the basis for the large-scan-feed network. The proposed structure offers scanning from -47 to 46 as the frequency changes from 3 GHz to 9 GHz. In [21], using active element loading, the antenna array scans from -9° to -30° with a gain equivalent to 8.3 dB to 9.7 dB over the operating range. In [22], a quad-band antenna is designed from an asymmetric E-CRLH TL and 50 Ω CPW feeding structure; the antenna achieved a maximum gain of 3.66 dBi. Four CRLH unit cells with a Butler matrix feeding network are designed in [23]. The radiation beam scan from -60° to 66° by changing the frequency from 3.7 GHz to 4.7 GHz. 20 microstrip MTM unit cells are designed in [24], and a continuous scan angle of 140° over the 3.80–5.25 GHz band with a maximum gain of 11.7 dB is achieved. In [25], a pattern diversity antenna is proposed. By controlling the CRLH - dispersion curve, the antenna realizes a broadside pattern and an omnidirectional pattern in the operated band.

This research introduces a novel MTM antenna array, providing high gain and bandwidth across the operating spectrum. The proposed array consists of an asymmetric CRLH unit cell combined with a third-order Hilbert curve structure. The dual-band antenna array operates from (3.3 to 4.2) GHz in the forward direction with a maximum gain of 7.24 dBi and (4.8 to 5.9) GHz in the backward direction with a maximum gain of 3.69 dBi, with S_{11} <= -15 dB along with the operating bands.

First, antenna geometrical details are discussed in section II. Then, simulation and parametric study are given in section III, where the methodology and procedure steps are explained. Next, comparing with the other research is discussed in section IV, where the study's significance and novelty are explained; at last, the conclusion is discussed in section V.

II. Antenna Geometrical Details

A. CRLH-MTM Design

Fig. 2 shows a T-symmetric CRLH-MTM represented interdigital capacitors (I_{DC}) and stub inductors printed on an FR-4 substrate with a relative dielectric constant ε_r=4.3 and a thickness subh=1.57 mm. The interdigital capacitor consists of 10 fingers with 10 mm length and 0.15 mm width, spaced by 0.1mm. The stub structure is structured as an inverted cross to avoid via use. Thus, the effects of high losses due to via introduction would be eliminated significantly [26] without increasing antenna design size or complexity. In addition, as seen in Fig. 2, a gap is introduced to the CRLH structure to create a capacitive filter effect to enhance the antenna bandwidth-gain product by suppressing the surface wave on the patch edges [27].

The unit cell is centred in the plane defined by the stub axis, representing a T-network consisting of two impedance branches with $2C_L$ and $L_R/2$ values and the admittance branch with L_L. and C_R values, see Fig. 1(b). The left-handed parameters are represented by I_{DC} and stub inductors. In contrast, the right-handed parameters are formed due to the circuit's parasitic interactions that increase with increasing frequency [28]. The magnetic field causes the parasitic inductance due to the surface current motion on the capacitor digits. At the same time, the parasitic capacitance is caused by the electric field gradients between the ground and the traces [29], see Fig. 2(b).

B. MTM Defects

The proposed MTM defects are etched from the antenna ground plane to eliminate the surface wave diffraction from the patch edges on the substrate. Nevertheless, reducing interference from the surface current at the ground plane [30]. The proposed MTM defects are structured from two

consequent 1D arrays, as seen in Fig. 3. The first array is consistent with 9-unit cells of the Hilbert curve etched from 14 mm^2 area from the ground plane, as seen in Fig. 3(a). The other array is introduced to fill the space between the first array unit cells with the number of elements of 8-unit cells. Each unit cell of the second array fills an area of 7 mm^2. Such a combination produces two stopbands, as seen in Fig. 3.

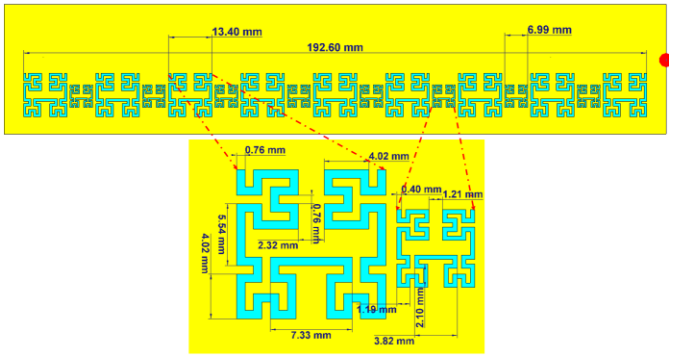

Fig. 3. The proposed MTM defect arrays.

A capacitive gap is formed between neighbouring cells in this array type, given by the following relationship [31]

$$c = \frac{p\varepsilon_o(1+\varepsilon_r)}{\pi}\cosh^{-1}\frac{p+g}{g} \quad (1)$$

The MTM defect shows capacitive behaviour, so it acts as a high-pass filter that allows high frequencies to pass through and prevents low frequencies [32, 33]. In addition, each cell is considered balanced with respect to the stub length, in which the capacitive effect is equal on both sides. The Hilbert cell represents the etched layer from the ground plane for this design. It is worth mentioning that the size and number of the Hilbert curve are chosen according to the size of the assumed MTM structure and the maximum size of the antenna. Thus, the capacitive reactance among the adjacent cells has similar effects on the suppression of surface currents, and hence the reactance can be expressed by the following relationship:

$$xc = \frac{1}{2\pi f c_{gap}} \quad (2)$$

III. Simulation and Discussion

This section used the CST software tool to analyze and simulate the antenna design parameters based on the finite integral technique [34]. The analysis and simulation are divided into the following parts:

A. CRLH-Unit Cell Performance

A detailed study is conducted on the CRLH to realize the effects of the antenna geometrical details on the equivalent circuit. As seen in Fig. 4, the CRLH was created using four parts: A transmission line, an inter-digital capacitor with ten fingers each, a T-stub inductor as a capacitive tuner, and the 3rd-order Hilbert curve. S-parameters are calculated separately for each case, as shown in Fig. 5. Finally, the CRLH structure is attached to a one-port transmission line with four models: model#1, model#2, model#3, and model#4.

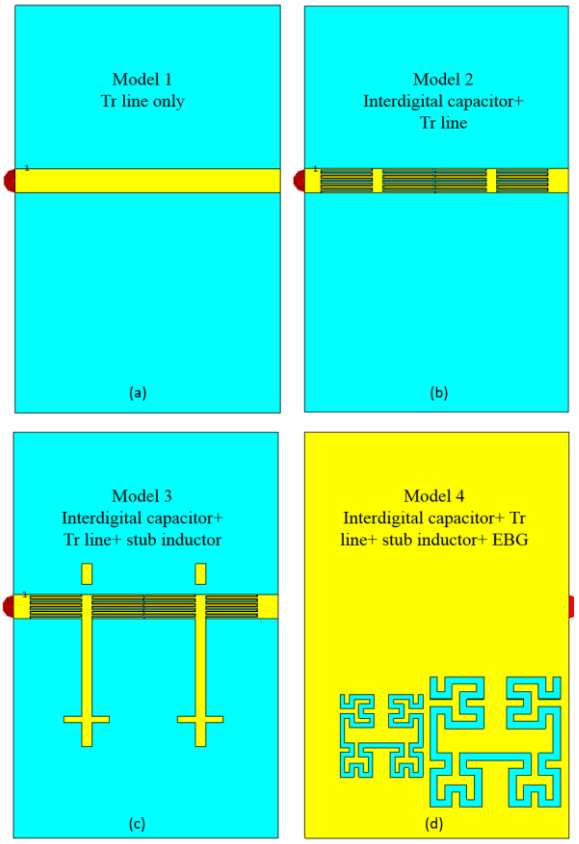

Fig. 4. Design models; (a) model 1 (b) model 2 (c) model 3 (d) model 4.

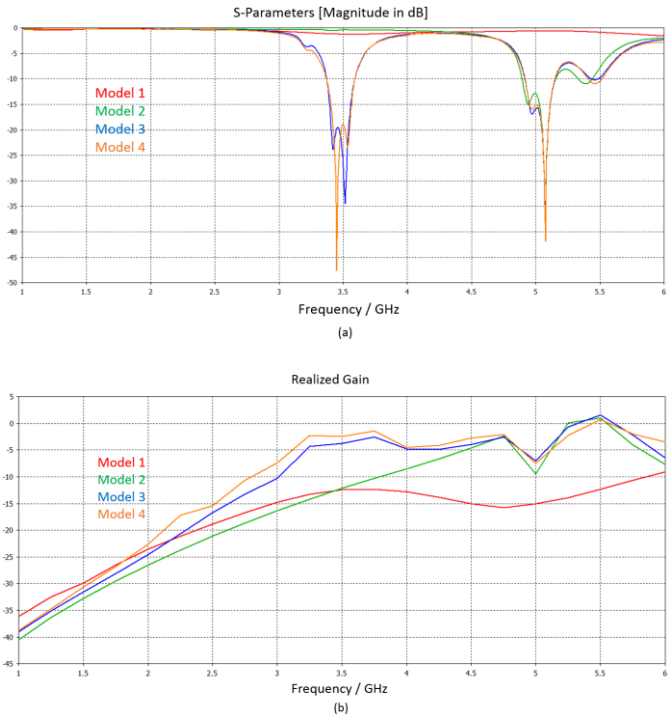

Fig. 5. CRLH-models Performance (a) S_{11} parameters and (b) realized gain.

The results show the influence of the unit cell components on the gain and frequency bands. The interdigital capacitor introduction creates a resonant frequency at 5 GHz. In addition, the T-stub inductor creates a double resonant frequency at 3.5 GHz and 5.5 GHz. At the same time, the Hilbert curve structure considerably increases the matching as it compensates for the via of the original design to allow current flow between the proposed CRLH and the ground plane. In addition, it cooperates with the substrate that generates losses, representing a feature that allows electric current to pass through and move between the radiator and the ground plane, enhancing the impedance bandwidth and gain, as illustrated in Fig. 5. The gain reached 0.7 dBi in the backward direction at 5.5 GHz.

B. CRLH-MTM Array Performance

Fig. 6(a) shows the final antenna design structure after reaching the optimum dimensions. Then, in Fig. (6b-6c), S_{11} parameters and the proposed antenna gain spectra are presented. It is found that the proposed antenna provides S_{11}<=-15 dB with a maximum gain of 7.24 dBi and 3.74 dBi in the forward-backwards directions, respectively. In addition, it is good to mention that the proposed antenna shows two main lobs at the frequencies of 5.6 GHz and 5.9 GHz by splitting the main lobs into two beams. Such a feature is desirable in many applications in the 5G systems of tracking more than one object simultaneously in the OFDM algorithms [35].

The design methodology flowchart of the proposed antenna that is considered for this work is shown in Fig. 7. This flow chart shows the considered antenna dimension that significantly influences the proposed antenna performance.

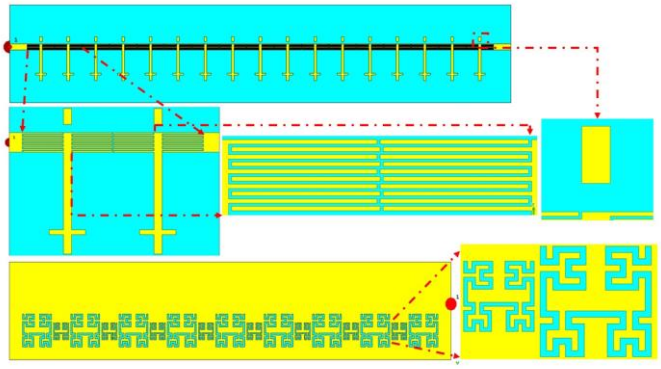

(a)

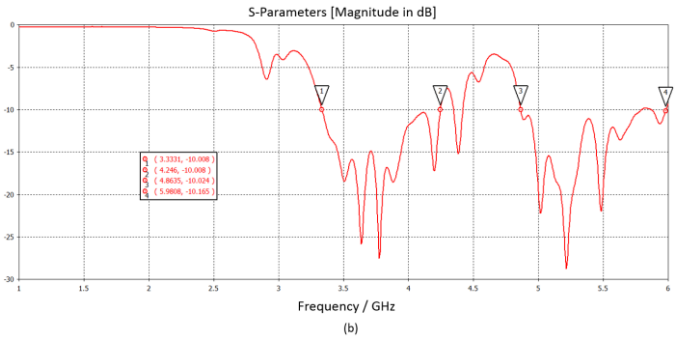

(b)

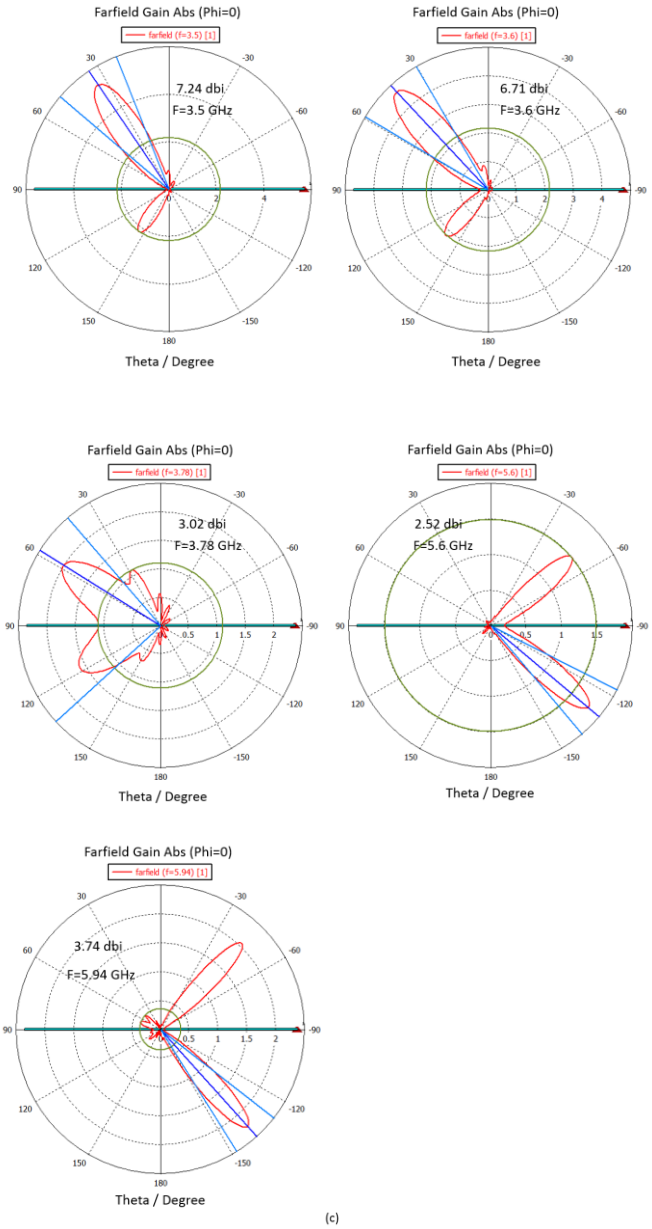

(c)

Fig. 6. Antenna performance: (a) antenna structure (b) S_{11} parameters (c) radiation patterns.

C. I_{DC} Parametric Influence

The authors conducted a parametric study to realize the effects of the proposed I_{DC} fingers on the antenna performance. The considered fingers are changed and varied from 1 to 5. S_{11} and gain spectra are calculated and presented in Fig. 8(a, b). The antenna performance changed. As the fingers increase, the losses decrease rapidly, which results in current distribution enhancements that improve the antenna gain-bandwidth product, as illustrated in Fig. 8. At 5.5 GHz the gain reached its maximum value for the backward direction.

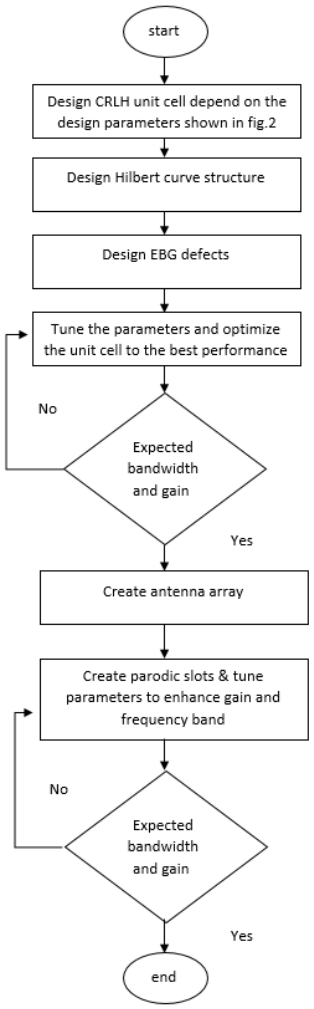

Fig. 7. Design methodology flowchart

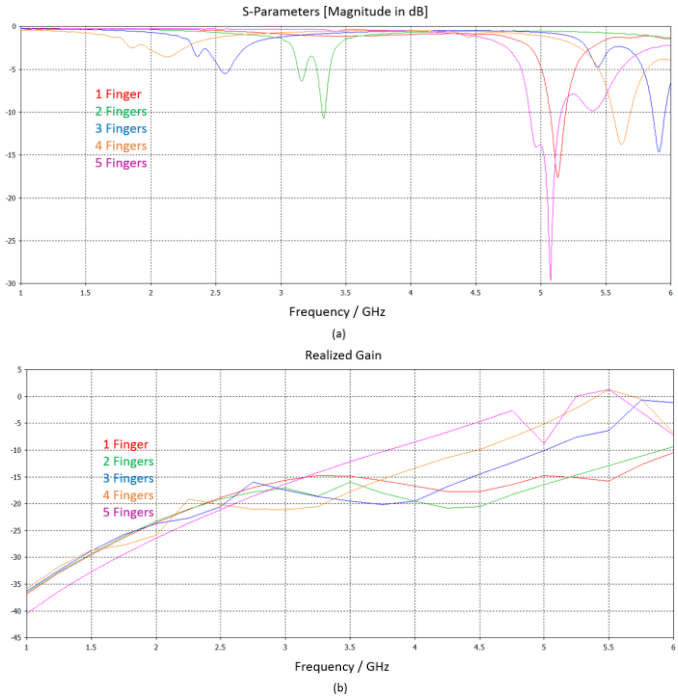

Fig. 8. I_{DC} parametric study: (a) S_{11} parameters and (b) realized gain.

D. *Slots Parametric Study*

A parametric study is conducted to clarify the impact of introducing antenna slots on the design and their importance in giving the desired results. The parametric study is conducted regarding the array's performance with and without slots. A comparison study in gain and S_{11} is made. It is found that the slots have an essential role in forming a wide bandwidth extending from 3.3 GHz to 4.24 GHz and 4.86 GHz to 5.98 GHz. In addition, a gain enhancement is achieved, especially in the forward direction of the radiation, as seen in Fig. 9.

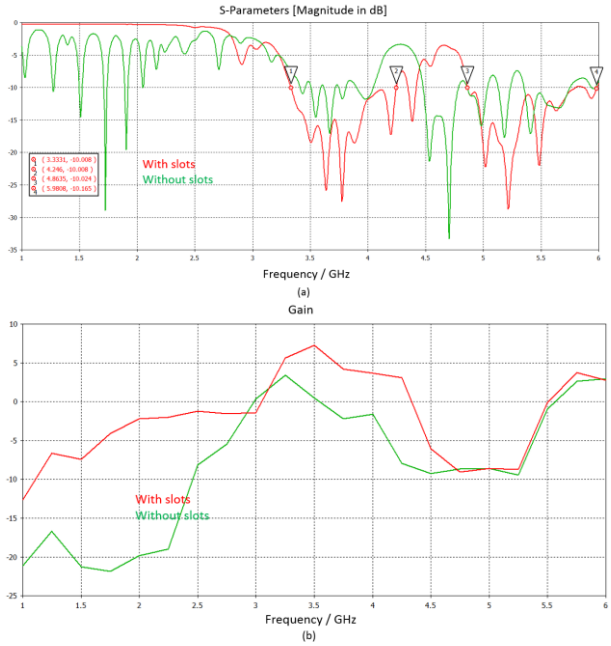

Fig. 9. Slots effects: (a) S_{11} parameters and (b) Gain.

E. *T-Stub Parametric Study*

In this part, the effects of the T-stub inductor were studied. First, the dimensions of the inductance are changed from 12 mm to 18 mm, as seen in Fig. 10. An improvement in the gain for the forward and backward directions is observed when the T-stub dimensions increase. Maximum gain is observed at 5.5 GHz. The T- shape at the end of the inductor significantly creates a frequency resonance at 3.5 GHz with S_{11} less than -35 dB. As the proposed T-Stub worked as a small size radiator provides a spreading in the electric current with a high-power distribution, which ensures the generation of a frequency band at 3.5 GHz.

F. *Effects of MTM Defects*

This section fully studies the effects of MTM defects on antenna performance. Two cases are considered: The first is the design with MTM defects and the second without MTM defects. The gain and bandwidth variations are evaluated for each case. As depicted in Fig. 11, the proposed MTM effects on the antenna bandwidth are found to be enhanced in the forward direction (3.3 GHz - 4.2 GHz and 4.3 GHz - 4.4 GHz)

to the backward direction (4.8 GHz - 5.9 GHz) with a maximum gain equal to (7.24 dBi, 3.74 dBi), respectively.

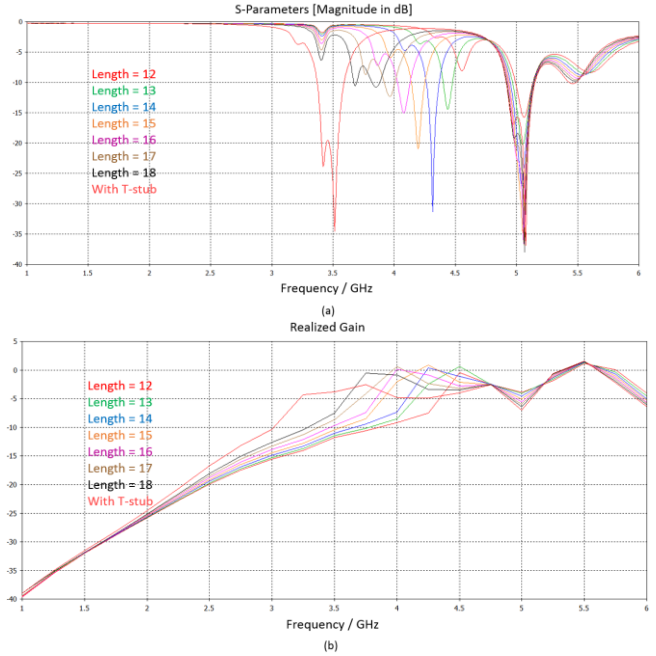

Fig. 10. T-Stub effects: (a) S_{11} parameters (b) realized gain.

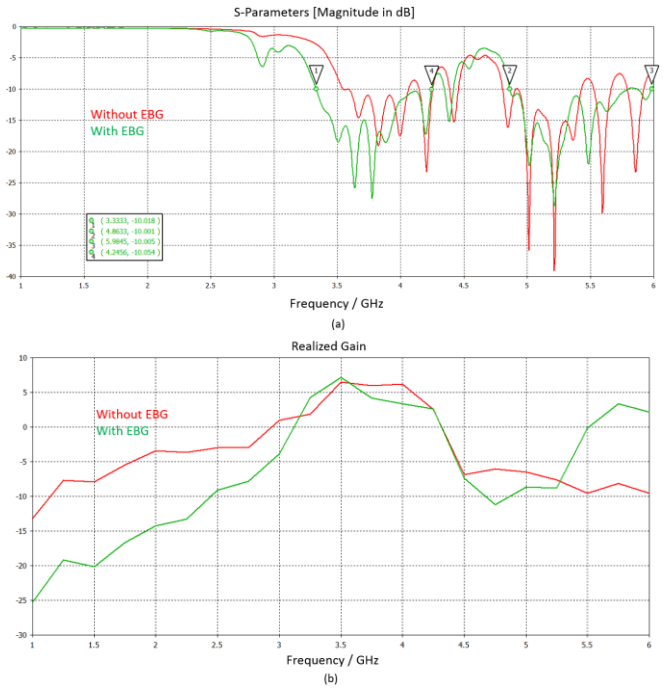

Fig. 11. EBG defects: (a) S_{11} parameters and (b) gain spectra.

IV. Reconfigurable Antenna Simulation Study

MTMs are resonant structures with unusual constitutive parameters depending on the resonance frequency. The material has positive constitutive properties at frequencies lower than the resonant frequency. In contrast, at frequencies higher than the resonant frequency, the material has negative constitutive parameters, and thus the material shows different behaviours depending on the operating frequency range [36, 37]. However, operating frequencies must be fixed and unchanged for most practical wireless applications. As a result, the metasurface must be reconfigurable to achieve multi-function properties. The frequency of interest can be changed by changing the bias voltage; thus, different MTM properties can be obtained at a fixed frequency [38].

This research proposes an MTS created through arranged periodic CRLH MTM cells separated by periodic slots with a gap in each inductor. To realize a reconfigurable metasurface, one PIN diode is inserted into the gap of each unit cell, as shown in Fig. 12(a). The equivalent circuit model in the forward and reverse biased state for the PIN diode are shown in Fig. 12(b) and (c) [39].

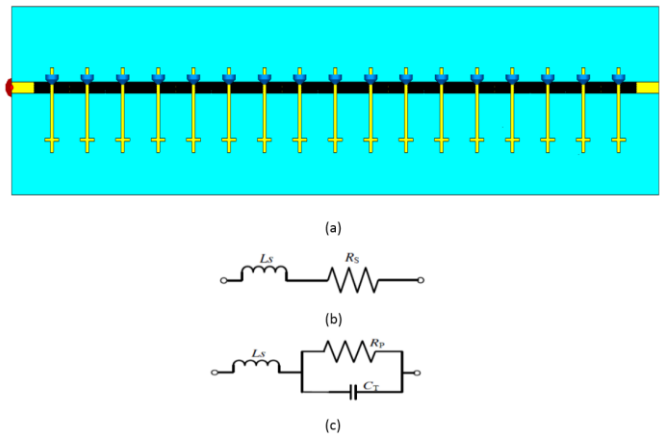

Fig. 12. Antenna structure: (a) 3D antenna structure, (b) PIN diode equivalent circuit OFF-state, and (c) ON-state.

By changing the state of the PIN diodes, the antenna beam direction varies from 34° to 42° at 3.5 GHz. Table I considers an input sequence to the PIN diodes; the antenna gain and beam direction variation are listed. In Fig. 13, S_{11} spectra and the radiation patterns at 3.5 GHz are calculated at different switching scenarios.

TABLE I
PIN Input Sequence

Input sequence	gain	Main lobe direction
00000000000000000	7.25	34
11111111100000000	6.78	40
00000000111111111	6.64	38
11000000000000000	7.23	35
11110000000000000	7.19	36
11111100000000000	7.13	37
11111111000000000	6.88	39
11111111111100000	6.72	41
11111111111111000	6.49	42

V. Comparison with the Latest Research

The following table summarises the most recent research in an area of interest and compares it to the proposed work.
Finally, the proposed design's novelty lies in a nine-cell antenna design that achieves a gain equivalent to 29 cells of the original design [40]. VIA was used in the original design to achieve losses in the original substrate, Roger, thus allowing surface current to pass between ground level and the radiator to create the parasitic effects needed to generate a CRLH unit cell. Here, VIA is replaced by a fractal technology that contributes with a low-cost, high-loss substrate, FR-4, to

achieve this interaction. Furthermore, this lossy substrate contributed with the fractal technology to generate a permeability that allows electric current to pass between the ground plane and the radiator. In other words, the VIA used with a high-cost substrate, Roger, was replaced by fractal technology with a low-cost substrate [FR-4] to achieve better performance with higher gain and higher bandwidth. The importance of the design lies in configuring an antenna of small size, low- cost and low- complexity to achieve requirements such as high bandwidth, good gain, and scanning capability that extends from the forward to the backward direction with a scanning capability of 8° at a fixed frequency. Therefore, this design is found to be suitable for 5G applications. Furthermore, the design can be extended and improved to create an array suitable for MIMO applications.

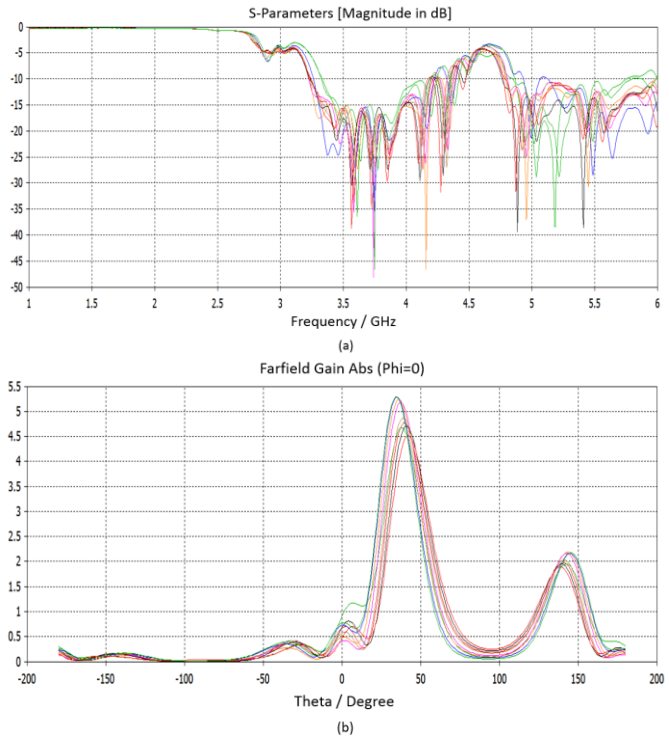

Fig. 13. Reconfigurable parametric study at 3.5 GHz (a) s_{11} parameter (b) radiation pattern.

TABLE II
COMPARISON WITH THE LATEST RESEARCH

Ref	Antenna-size (mm^2)	Frequency range (GHz)	Peak gain (dBi)	Bands	Scanning range(deg.)
[16]	250×100	4-6	10	Wideband	15 and 55
[20]	----------	3-9	5	Wideband	-47 to 46
[21]	15×440	3.4-3.7	8.3	single band	-9° to -30°
[22]	57.2×31.2×1.6	2.45-5.5	-8.12, -1.31,1.46, 3.66	Four-bands	----------
[23]	137×101	3.7-4.7	11.8	----------	-60° to 66°
[24]	24×6	3.80-5.25	11.7	----------	140°
[25]	80×80	2.49/3.45	4, 6	Dual band	----------
[40]	170.8*40	3.9	8	---------	75°-122°
This work	40×204	3.3-4.2/4.8-5.9	7.24, 3.74	Dual-band	34° to 42°

VI. CONCLUSION

In this paper, an antenna was designed with new technology. At first, a regular microstrip line was created. Next, a series I_{DC} and an S_I were added to form a CRLH-MTM. Finally, a Hilbert curve structure was added to compensate for the VIA. As a result, the antenna works with a dual bandwidth extending from (3.3 to 4.2) (4.86 to 5.98) GHz with good gain along the operated bands. Furthermore, the antenna doesn't require a specialized feeding structure or a phase shifter, which reduces its size and complexity; therefore, the design is characterized by its simplicity and high performance and the possibility of scanning capability, making it suitable for 5G applications.

REFERENCES

[1] J.K. Ali, E.M. Abdul-Baki, M.H. Hammed: A multiband fractal dipole antenna for wireless communication applications, Engineering & Technology Journal, Vol.28, No.10, pp.2043-2053, 2010.

[2] B.S. Bashar, M.M. Ismail, A.S.M. Talib: Optimize Cellular Network Performance Using Phased Arrays, In IOP Conference Series: Materials Science and Engineering, Vol. 870, No(1), p. 012128, June. 2021.

[3] R. Noumi, J. Machac, A. Gharsallah: Tunable Liquid Crystal MTM SIW LWA for continuous scanning at fixed frequency, In IEEE 19th Mediterranean Microwave Symposium (MMS), Vol.2019, 2019.

[4] T. Saeidi, I. Ismail, W.P. Wen, A.R. Alhawari, A. Mohammadi: Ultra-wideband antennas for wireless communication applications, International Journal of Antennas and Propagation, Vol.2019, 2019.

[5] H.S. Ahmed, J.K. Ali, A.J. Salim: Design of fractal-based bandstop filter for microwave radiation leakage reduction, Engineering and Technology Journal, Vol.35, No.1, pp.16-23, 2017.

[6] P.S. Chindhi, G.B. Kalkhambkar, H.P. Rajani, R. Khanai: A brief survey on metamaterial antennas: Its importance and challenges, Futuristic Communication and Network Technologies, pp.425-432,2022.

[7] H. Shahraki, K. Afrooz, A. Hakimi: Dual extended composite right/left-handed transmission line metamaterial, International Journal of RF and Microwave Computer-Aided Engineering, Vol.28, No.5, p. e21247,2018.

[8] M.A. Abdalla, Z. Hu: A review on novel magnetic properties of metamaterials CRLH devices, Journal of Engineering Science and Military Technologies, Vol.2, No.4, p. 153-160, 2018.

[9] T. Kenion, N. Yang, C. Xu: Dielectric and mechanical properties of hypersonic radome materials and metamaterial design: A review, Journal of the European Ceramic Society, Vol.42, No.1, p. 1-17, 2022.

[10] Z. Wang, Y. Dong: Miniaturized RFID reader antennas based on CRLH negative order resonance, IEEE Transactions on Antennas and Propagation, Vol.68, No.2, p. 683-696, 2019.

[11] C. Caloz, T. Itoh: Novel microwave devices and structures based on the transmission line approach of meta-materials, in IEEE MTT-S International Microwave Symposium Digest, Vol.1, pp. 195-198, 2003.

[12] M. Mohammadi, J. Ghalibafan: Unbalanced CRLH behavior of ferrite-loaded waveguide operated below cutoff frequency, Waves in Random and Complex Media, Vol.32, No.2, p. 755-770, 2022.

[13] K. Ghosh, S. Das: CRLH-TL Based Reconfigurable Antennas with Multiple Parameter Reconfigurability, IEEE Transactions on Antennas and Propagation, 2022.

[14] A.H. Jabire, A. Ghaffar, X.J. Li, A. Abdu, S. Saminu, M. Alibakhshikenari, F. Falcone, E. Limiti: Metamaterial based design of compact UWB/MIMO monopoles antenna with characteristic mode analysis, Applied Sciences, Vol.11, No.4, p.1542, 2021.

[15] M. Alibakhshikenari, B.S. Virdee, C.H. See, R.A. Abd-Alhameed, F. Falcone, E. Limiti: High-isolation leaky-wave array antenna based on CRLH-metamaterial implemented on SIW with±30° frequency beam-scanning capability at millimetre-waves, Electronics, Vol.8, No.6, p.642, 2019.

[16] H. Singh, B.S. Sohi, A. Gupta: A compact CRLH metamaterial with wide band negative index characteristics, Bulletin of Materials Science, Vol.42, No.4, p. 1-11, 2019.

[17] J.S. Kasim, M.S.M. Isa, Z. Zakaria, M.I. Hussein, M.K. Mohsen: Radiation beam scanning for leaky wave antenna by using slots,

Telecommunication Computing Electronics and Control, Vol.18, No.3, pp.1237-1242, 2020.
[18] M. Alibakhshikenari, B.S. Virdee, A. Ali, E. Limiti: Extended aperture miniature antenna based on CRLH metamaterials for wireless communication systems operating over UHF to C-band, Radio Science, Vol.53, No.2, pp.154-165, 2018.
[19] I. Slomian, K. Wincza, S. Gruszczynski: Composite right-/left-handed leaky-wave antenna utilizing coupled-line sections, Journal of ElEctromagnEtic WavEs and applications, Vol.32, No.6, p. 768-780, 2018.
[20] B.F. Zong, H.Y. Zeng, F. Wu, G.M. Wang, L. Geng: Wide-angle frequency-scanning array antenna using dual-layer finger connected interdigital capacitor based CRLH unit cell, IEEE Access, Vol.9, pp.35957-35967, 2020.
[21] H.X. Li, Y.J. Zhou: Dual-polarized Fixed-frequency Beam Scanning Leaky-wave Antenna for 5G Communication, The Applied Computational Electromagnetics Society Journal (ACES), Vol.36. No.7, p. 858-864, 2021.
[22] H.B. Chu, H. Shirai: A compact metamaterial quad-band antenna based on asymmetric E-CRLH unit cells, Progress In Electromagnetics Research C, Vol.81, p. 171-179, 2018.
[23] X. Ding, Y.M. Wu, F.L. Jin, Z.P. Wang, B.Z. Wang: A SIW Leaky-Wave Beam Scanning Array, In 2019 IEEE International Symposium on Antennas and Propagation and USNC-URSI Radio Science Meeting, pp. 2067-2068.
[24] Y.L. An, Y.L. Tan, H.B. Zhang, G.C. Wu: Double-layered microstrip metamaterial beam scanning leaky wave antenna with consistent gain and low cross-polarization, Applied Physics A, Vol.123, No.12, pp.1-8, 2017.
[25] J. Zhang, S. Yan, G.A. Vandenbosch: Realization of dual-band pattern diversity with a CRLH-TL-inspired reconfigurable metamaterial, IEEE Transactions on Antennas and Propagation, Vol.66, No.10, p. 5130-5138, 2018.
[26] M. Ameen, A. Mishra, R.K. Chaudhary: Dual-band CRLH-TL inspired antenna loaded with metasurface for airborne applications, Microwave and Optical Technology Letters, Vol.63, No.4, p. 1249-1256, 2021.
[27] R. Cicchetti, E. Miozzi, O. Testa: Wideband and UWB antennas for wireless applications: A comprehensive review, International Journal of Antennas and Propagation, 2017.
[28] M. Alibakhshikenari, B.S. Virdee, C.H. See, R.A. Abd-Alhameed, F. Falcone, E. Limiti: High-gain metasurface in polyimide on-chip antenna based on CRLH-TL for sub-terahertz integrated circuits, Scientific reports, Vol.10, No.1, pp.1-9, 2020.
[29] Y.M. Madany, D.A. Mohamed, B.I. Halim: Analysis and design of microstrip antenna array using interdigital capacitor with CRLH-TL ground plane for multiband applications, in The 8th European Conference on Antennas and Propagation, pp. 922-926, 2014.
[30] D.M. Elsheakh, H.A. Elsadek, E.A. Abdallah: "Antenna designs with electromagnetic band gap structures" in Metamaterial, 2012, p. 403-473.
[31] P.P. Bhavarthe, S.S. Rathod, K.T. Reddy: A compact two via slot-type electromagnetic bandgap structure, IEEE Microwave and Wireless Components Letters, Vol.27, No.5, p. 446-448, 2017.
[32] M.A. Habib, M.N. Jazi, A. Djaiz, M. Nedil, T.A. Denidni: Switched-beam antenna based on EBG periodic structures, In 2009 IEEE MTT-S International Microwave Symposium Digest, pp. 813-816, 2009.
[33] H.T. Ziboon, J.K. Ali: Compact dual-band bandpass filter based on fractal stub-loaded resonator, in 2017 Progress In Electromagnetics Research Symposium-Spring (PIERS) pp. 1815-1819, 2017.
[34] CST program. 2022; Dassault Systèmes:[Available from: https://www.3ds.com/products-services/simulia/products/cst-studiosuite/?utm_source=cst.com&utm_medium=301&utm_campaign=cst.
[35] F. Maschietti: "Decentralized coordination methods for beam alignment and resource allocation in 5G wireless networks" Sorbonne Université, 2019.
[36] Q. He, S. Sun, L. Zhou: Tunable/reconfigurable metasurfaces: physics and applications, Research, 2019.
[37] J.M. Rasool: MIMO Antenna System Using Orthogonally Polarized Ultra Wide Band Antennas With Metamaterial, Engineering and Technology Journal, Vol.28, No.24, 2010.
[38] Q. He, S. Sun, S. Xiao, L. Zhou: High-efficiency metasurfaces: principles, realizations, and applications, Advanced Optical Materials, Vol.6, No.19, p.1800415, 2018.
[39] S. Chaimool, T. Hongnara, C. Rakluea, P. Akkaraekthalin, Y. Zhao, :Design of a PIN diode-based reconfigurable metasurface antenna for beam switching applications, International Journal of Antennas and Propagation, 2019.
[40] C. Caloz, T. Itoh, A. Rennings: CRLH metamaterial leaky-wave and resonant antennas, IEEE Antennas and Propagation Magazine, 2008. Vol.50, No.5, p. 25-39, 2008.

Marwa M. Ismail received her B.Sc. degree in the electrical engineering department (2008), postgraduate M.Sc. degree in electrical and electronic engineering department (2012) from University of technology, Baghdad, Iraq. Now, she is completing her PhD at the University of Technology, Baghdad, Iraq, and is currently in the research phase. Her research areas include smart antennas and beamforming, design, modeling and testing of metamaterial structures for microwave applications, design, and analysis of microstrip antennas for mobile radio systems.

Taha A. Elwi received his B.Sc. degree in electrical engineering and M.Sc. degree in laser and optoelectronics engineering at NUB. He obtained his PhD degree in the system engineering and science department, University of Arkansas. His research areas include wearable antennas, smart antennas, metamaterial, microstrip antennas and MIMO.

Ali J. Salim received his B.Sc. degree in electrical engineering and a M.Sc. degree in communication engineering, UOB, Iraq and PhD degree in communication engineering, UOT, Iraq. He has published over 45 papers on printed antennas, wearable textile antenna design, and filter design (SIW) technology for microwave systems, and MIMO.